

Supermassive Neutron Stars Rule Out Twin Stars

Jan-Erik Christian^{1,*} and Jürgen Schaffner-Bielich^{1,†}

¹*Institut für Theoretische Physik, Goethe Universität Frankfurt,
Max von Laue Strasse 1, D-60438 Frankfurt, Germany*

We investigate the implications of a hypothetical $2.5 M_{\odot}$ neutron star in regard to the possibility of a strong phase transition to quark matter. We use equations of state (EoS) of varying stiffness provided by a parameterizable relativistic mean field model transitioning in a first order phase transition to quark matter with a constant speed of sound. We find a strong connection between the discontinuity in energy density and the maximal mass generated by the EoS. We demonstrate, that high maximal masses cannot be realized for large discontinuities in energy density, which are necessary for visible twin stars, especially for soft EoSs. As a result twin stars and maximal masses of $M_{max} \gtrsim 2.2 M_{\odot}$ are mutually exclusive.

I. INTRODUCTION

The global properties of neutron stars are uniquely related to the bulk properties of the matter inside, which is given by the equation of state of nuclear matter. The fundamental theory of strong interactions, quantum chromodynamics QCD, can not be solved at present at the high densities encountered inside neutron stars. So one has to resort to observations and detailed modeling to learn more about the equation of state at high densities.

There are currently three main methods of constraining the equation of state of neutron stars. Most commonly used is the mass constraint of about $2 M_{\odot}$ [1–5], which is the mass of the most massive pulsars measured today. Every viable EoS has to be able to generate a maximal mass higher than this constraint. The radius of a neutron star can be used as a constraint for the EoS as well, via the placement of the neutron star in a mass-radius diagram. NICER [6–8] provides a comparatively precise radius measurement of the millisecond pulsar PSR J0030+0451. With the increased usage of gravitational wave detectors like LIGO the tidal deformability of neutron stars can be used as an additional constraint. It can be measured from gravitational waves emitted by a binary neutron star inspiral [9–12]. In the case of GW170817 the measurement, points to soft EoSs that feature more compact neutron stars [12–17]. Recently, in the gravitational wave event GW190814 a merger of a black hole with an unknown $2.59^{+0.08}_{-0.09} M_{\odot}$ compact object was observed [18]. In light of this discovery we investigate the implications of a hypothetical neutron star with the mass of this unknown object for hybrid and twin star equations of state.

A common type of EoS to describe neutron stars is the relativistic mean field model [19–26]. However, due to the high pressures at the center of a neutron star a quark matter core with a hadronic crust instead of a purely hadronic EoS could be present. This configuration is called a hybrid star [27–34]. The phase transition from

hadronic matter to quark matter can lead to a discontinuity in the mass-radius relation. This gives rise to the phenomenon known as twin stars, where two neutron stars have the same mass, but different radii [35–46]. Hybrid and twin stars tend to be rather compact, which is in good agreement with GW170817 [12–17]. However, it implies a soft hadronic EoS, which can come into conflict with the mass constraint. In this work we will use the parameterizable relativistic mean field equation of state in the form presented by Hornick et al. [26] and combine it with a constant speed of sound (CSS) approach for quark matter [47–49] via a Maxwell-construction. This ansatz gives us the opportunity to vary the parameters and apply the hypothetical GW190814 constraint in a more generalized way. We also discuss the $2.14^{+0.10}_{-0.09} M_{\odot}$ pulsar mass constraint from Cromartie et al. [4]. We find, that EoSs featuring twin stars and masses of $M_{max} \gtrsim 2.2 M_{\odot}$ are mutually exclusive. However hybrid stars without a discontinuity in the mass radius relation are still viable and can even reach maximal masses of $M_{max} > 2.5 M_{\odot}$, as for example Tan et al. [50] discuss.

II. THEORETICAL FRAMEWORK

A. Equation of State

1. Hadronic Equation of State

The relativistic mean-field model we use here was introduced by Todd-Rudel et al. [51] (see also: Chen et al. [52]) and is a generalized relativistic mean field approach with the main advantage, that the slope parameter L , the symmetry energy J and the effective nucleon mass m^*/m can be easily adjusted. Hornick et al. [26] additionally constrain the parameters using the constraints from χ EFT for densities up to $1.3 n_0$ [53]. By comparing the different EoSs with the allowed band from χ EFT they find, that only values of $40 \text{ MeV} \leq L \leq 60 \text{ MeV}$ and $30 \text{ MeV} \leq J \leq 32 \text{ MeV}$ are allowed.

The choices of L and J have no significant impact on the mass radius relation as shown in ref. [26]. This allows us to fix the values $L = 60 \text{ MeV}$ and $J = 32 \text{ MeV}$

* christian@astro.uni-frankfurt.de

† schaffner@astro.uni-frankfurt.de

in a way, that provides the largest range in m^*/m from $m^*/m = 0.55$ to $m^*/m = 0.75$. Note that the stiffness of an EoS relates to the value of m^*/m [54]. The lower the effective mass parameter, the stiffer is the EoS.

2. Phase Transition

We consider a first order phase transition at high baryonic densities from hadronic to quark matter EoS. For the hadronic matter we use the parameterized EoS (see previous section), while the constant speed of sound approach [39, 48, 49] in the form introduced by Alford et al. [48] is employed for the quark matter. This means, the entire EoS is given as:

$$\epsilon(p) = \begin{cases} \epsilon_{HM}(p) & p < p_{trans} \\ \epsilon_{HM}(p_{trans}) + \Delta\epsilon + c_{QM}^{-2}(p - p_{trans}) & p > p_{trans} \end{cases} \quad (1)$$

where p_{trans} is the transitional pressure and $\epsilon_{HM}(p_{trans})$ the energy density at the point of transition. The discontinuity in energy density at the transition is $\Delta\epsilon$. In order to achieve the stiffest possible EoSs and thus the greatest possible range of mass-radius relations we set $c_{QM} = 1$ using natural units.

B. Classification of Twin Stars

A first order phase transition can give rise to the phenomenon of "twin stars", which are neutron stars with identical mass, but different radii [35–42, 44]. When analyzing such EoSs it can be useful to classify the twin star solutions into four distinct categories, as described in [44]. We refer to the maximum of the hadronic branch as the first maximum M_1 and the maximum of the hybrid branch as the second maximum M_2 in a twin star mass-radius relation. The mass value of the first and second maximum can be related to values of p_{trans} and $\Delta\epsilon$ respectively [44]. The shape of the second branch is correlated with the value of p_{trans} , while its position is strongly influenced by the value of $\Delta\epsilon$. High values of p_{trans} lead to high masses in the first maximum and flat second branches. Low values of $\Delta\epsilon$ lead to a second branch near the discontinuity (i.e. a high mass at the second maximum). Based on this observation the categories can be defined as:

- I:** Both maxima exceed $2 M_\odot$, which implies high values of p_{trans} and a nearly flat second branch. As a result the maximal mass of a category I case is usually a pure hadronic neutron star.
- II:** Only the first maximum reaches $2 M_\odot$, which again requires a high value of p_{trans} . The flat second branch is moved to lower values of mass and radius.
- III:** The first maximum is in the range of $2 M_\odot \geq M_{max1} \geq 1 M_\odot$, while the second maximum ex-

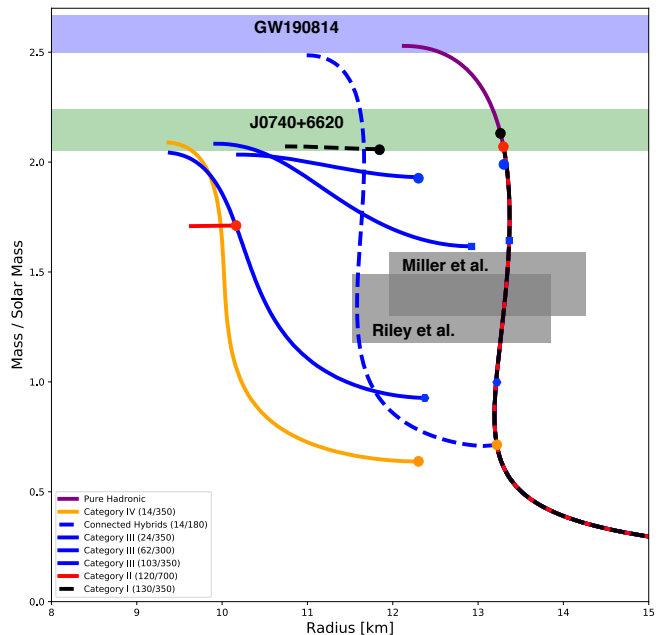


FIG. 1. Examples for category I (black dashed line), II (red dashed line), III (blue continuous lines) and IV (orange line) phase transitions for a hadronic base EoS with $m^*/m = 0.65$. For comparison the pure hadronic case was added as well (purple line), as well as an example of a connected second branch (dashed blue line). The values in parenthesis indicate the transitional pressure and the jump in energy density in units of MeV/fm^3 respectively. The point, where the first branch ends is dictated by the transitional pressure and indicated by a dot in color corresponding to the category. Additionally the NICER constraints [6, 7] (black shaded area), Cromartie constraint [4] (green shaded area) and the unknown compact object of GW190814 [18] (blue shaded area) were added. For the black shaded area only the stated values of the NICER constraint are shown, however the full error ellipses at the 2σ interval would still include the category IV example.

ceeds $2 M_\odot$. Accordingly, the transitional pressure is lower than in the previous categories and the second branch becomes steeper. The most massive star in these configurations is always a hybrid star.

IV: Like category III the second maximum exceeds $2 M_\odot$, however the first maximum is below even $1 M_\odot$. The second branch is at its steepest slope here.

Due to the quark matter dominated EoSs in category IV the hadronic part can be nearly arbitrarily soft and the combination can still reach $2 M_\odot$. Category I-III do not allow for effective masses of $m^*/m \geq 0.75$.

Examples for all four categories are provided in Fig. 1. The base hadronic EoS in this example is the parameterized relativistic mean field model with an effective mass of $m^*/m = 0.65$. Category I (dashed black line) and category II (red line) have their hadronic maxima close to each other. In general all values of p_{trans} in category II are also included in category I. The distinguishing factor is the higher jump in energy density for the category II cases, which moves the flat second branch further down.

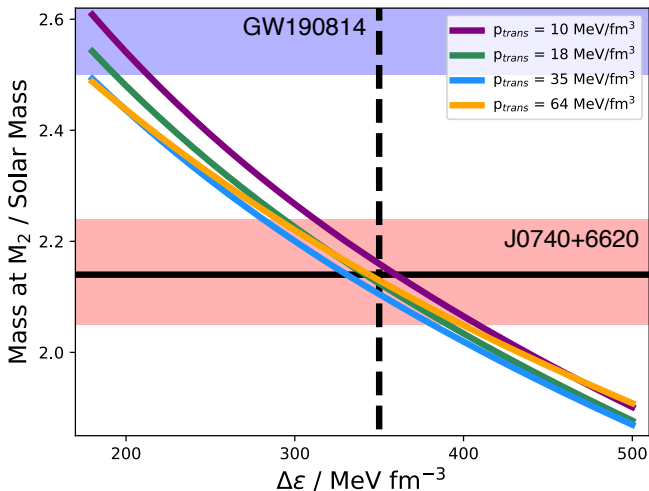


FIG. 2. The $m^*/m = 0.55$ case of the maximal hybrid star mass as a function of the jump in energy density for different transitional pressures. The case $p_{trans} = 64 \text{ MeV/fm}^3$ (orange) is incompatible with the LIGO measurement of GW170817 [17, 55]. The dashed black line indicates $\Delta\epsilon = 350 \text{ MeV/fm}^3$, which is the lowest value of $\Delta\epsilon$ that generates a mass gap of $\Delta M = \pm 0.1 M_\odot$ for all transitional pressures. The hypothetical neutron star participant of a GW190814 (shaded blue) is only realizable for smaller values of $\Delta\epsilon$, implying no viable mass gap. The solid horizontal black line represents the $2.14 M_\odot$ of J0740+6620 [4]. Only the $p_{trans} = 10 \text{ MeV/fm}^3$ case reaches this value at $\Delta\epsilon \leq 350 \text{ MeV/fm}^3$, suggesting, that only this case can support twin stars and a maximal hybrid star mass of $M_2 \geq 2.14 M_\odot$. However, when considering the error bar of the stated mass (red shaded area) all cases reach the limit.

Since category III contains the greatest variety of shapes we include three examples for this category (continuous blue lines): One at the lower limit of the transitional pressure, i.e. $M_1 \simeq 1 M_\odot$ ($p_{trans} = 24 \text{ MeV/fm}^3$), one at the upper limit, i.e. $M_1 \simeq 2 M_\odot$ ($p_{trans} = 103 \text{ MeV/fm}^3$) and one example from the mid-range ($p_{trans} = 62 \text{ MeV/fm}^3$). With decreasing transitional pressure the second branch becomes much steeper when compared to previous categories, until the category IV case (orange line) is nearly orthogonal to category I and II cases.

Fig. 1 also includes a connected hybrid star configuration with an early phase transition (dashed blue line). A connected branch has a kink at the point of transition and is realized for small values of $\Delta\epsilon$. Hybrid stars with a connected branch can reach higher masses than true twin star configurations, however the presence of a phase transition is hard to determine from mass-radius measurements.

III. TRYING TO RECONCILE STRONG PHASE TRANSITIONS WITH A HYPOTHETICAL $2.5 M_\odot$ NEUTRON STAR

A. The stiffest case

Since the case $m^*/m = 0.55$ is the stiffest possible hadronic equation in our model it will feature the most massive neutron stars. Therefore any cases excluded by this EoS due to an insufficient maximum mass are excluded for all cases $m^*/m > 0.55$ as well. For this reason we will consider $m^*/m = 0.55$ first.

Fig. 2 shows the masses at the hybrid star maximum M_2 , as they depend on the jump in energy density $\Delta\epsilon$ for the case $m^*/m = 0.55$. There is a correlation between M_2 and $\Delta\epsilon$. In our previous publication [17] we used the NICER measurement [6–8] at the 2σ level to constrain the minimal density at the core for strong phase transitions to $n \approx 1.4 n_0$. This corresponds to about $p_{trans} \geq 10 \text{ MeV/fm}^3$ for the $m^*/m = 0.55$ case used here (purple line in Fig. 2). The 1σ accuracy of the NICER radius constraint [6–8] corresponds to $n \approx 1.7 n_0$ [17] which is about $p_{trans} \geq 18 \text{ MeV/fm}^3$ for this EoS (green line in Fig. 2). The cases $p_{trans} = 35 \text{ MeV/fm}^3$ (blue line) and $p_{trans} = 64 \text{ MeV/fm}^3$ (orange line) are the middle and upper limit of category III phase transitions respectively. This means that those two cases correspond to maximal masses of about $2 M_\odot$ and about $1.5 M_\odot$ in the first branch. The $p_{trans} = 64 \text{ MeV/fm}^3$ is not compact enough to fit with the GW170817 measurement [55], but was included for completeness.

We considered a phase transition to be strong if the jump in mass between the hadronic maximum and the hybrid star minimum is larger than $0.1 M_\odot$. This is possible for every EoS in our model, if the discontinuity in energy density is $\Delta\epsilon \geq 350 \text{ MeV/fm}^3$ and a twin star branch is generated at all. The condition $\Delta\epsilon \geq 350 \text{ MeV/fm}^3$ is not a rigorous constraint, but a good approximation, as all cases $\Delta\epsilon = 350 \text{ MeV/fm}^3$ lead to $\Delta M \geq 0.1 M_\odot$, even if there are cases where a lower jump in energy density would be sufficient already. The case $p_{trans} = 10 \text{ MeV/fm}^3$ has a maximal mass of about $2.2 M_\odot$ at a discontinuity of $\Delta\epsilon = 350 \text{ MeV/fm}^3$. One of the most massive neutron stars known today [4] is indicated in Fig. 2 as a black vertical line at $2.14 M_\odot$ with a red shaded error bar of $^{+0.10}_{-0.09}$. All cases shown reach at least the 1σ error-bar for $\Delta\epsilon \geq 350 \text{ MeV/fm}^3$.

However, masses as large as the hypothetical $2.59^{+0.08}_{-0.09} M_\odot$ posed by GW190814 [18] would imply, that a strong phase transition that produces visible twin stars can not be realized in nature. Hybrid stars with a connected branch (i.e. cases with $\Delta\epsilon \leq 350 \text{ MeV/fm}^3$) could still fit the data. Category I and II of the $m^*/m = 0.55$ case contain maximal masses of, at most, $M_{max} \simeq 2.35 M_\odot$ with the maximal hybrid star mass being similar or lighter than the purely hadronic maximum. Since category I contains the highest possible maximal mass of all four twin star

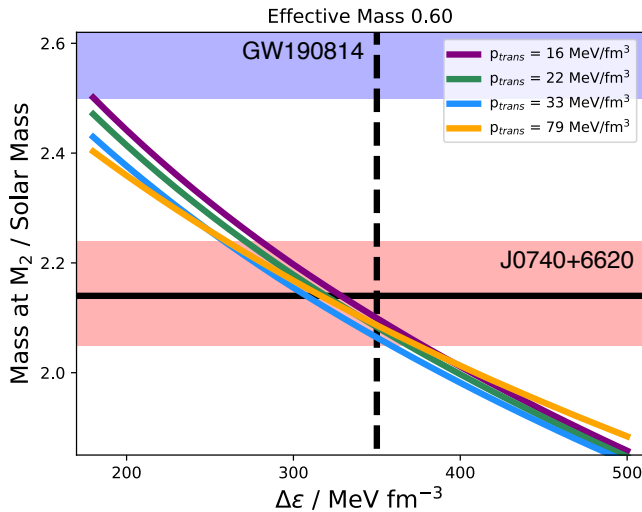


FIG. 3. Maximal hybrid star masses generated by different transitional pressures from category III and IV phase transitions of the $m^*/m = 0.60$ case. The $m^*/m = 0.60$ case contains lower values of M_2 when compared to the $m^*/m = 0.55$ case. However it is still possible to reach the lower limit of the error bar (shaded red) with all category III phase transitions at a energy density discontinuity larger than $\Delta\epsilon \geq 350 \text{ MeV/fm}^3$ (dashed line). No combination reaches a mass of $2.14 M_\odot$ (black vertical line) at $\Delta\epsilon \geq 350 \text{ MeV/fm}^3$.

categories and the $m^*/m = 0.55$ case contains the most massive stars it would follow, that a neutron star measurement of $M > 2.35 M_\odot$ would rule out twin stars. However, since the $m^*/m = 0.55$ case is too stiff to produce stars compact enough to match the GW170817 measurement without an early phase transition [17], category I and II configurations of this case are not compatible with this event. This means the category IV case of about $M_{max} \simeq 2.2 M_\odot$ is the highest possible mass a twin star configuration can reach.

B. Softer Cases

In this section we study the parameterizations with higher effective masses, i.e. softer nuclear EoSs. In Fig. 3-5 the purple line always represents the transitional pressure corresponding to $1.7n_0$, which we assume to be the minimal density necessary at the point of transition to generate mass-radius relations compatible with the recent NICER measurement [6–8] based on our previous work [17]. The low value of these transitional pressures places the mass-radius relations in category IV. The remaining three cases shown in each figure represent the lower limit (green line), a for the category representative example (blue line) and the upper limit (orange line) of category III respectively. As before we do not include categories I and II because the maximal mass for those categories is found in the first branch.

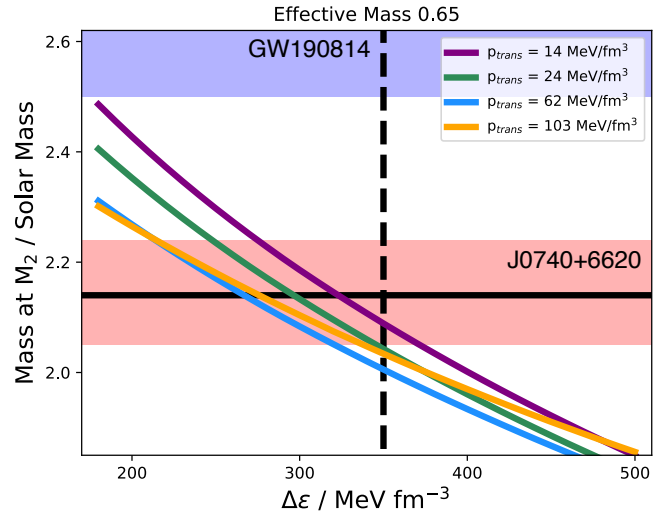


FIG. 4. Most transitional pressures of category III in the $m^*/m = 0.65$ case do not reach the pulsar mass limit of J0740+6620 at $\Delta\epsilon \geq 350 \text{ MeV/fm}^3$. Therefore only the cases where $p_{trans} \leq 24 \text{ MeV/fm}^3$ have a mass gap of $0.1 M_\odot$ and generate a mass value compatible with Cromartie et al. [4] at the 1σ interval.

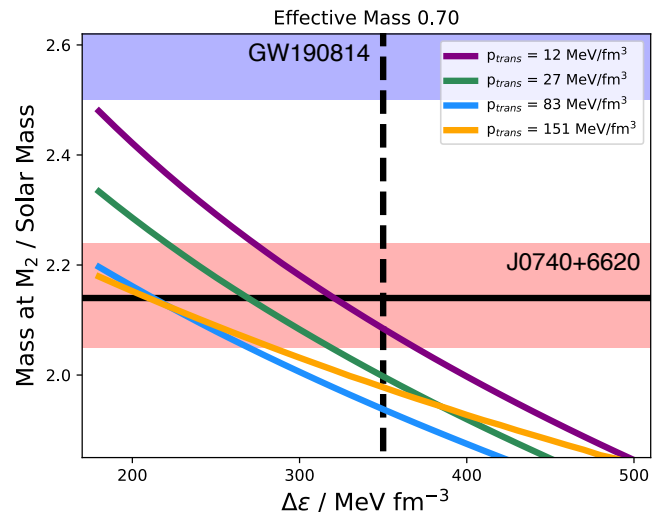


FIG. 5. For $m^*/m = 0.70$ only the category IV case $p_{trans} = 12 \text{ MeV/fm}^3$ allows for a configuration with $\Delta\epsilon \geq 350 \text{ MeV/fm}^3$ and a maximal hybridstar mass $M_2 \geq 2.05 M_\odot$. All other cases would not produce visible twin stars and the required hybrid star mass.

As expected an increase of the effective mass results in a decrease of the maximal hybrid star mass. Only transitional pressures of $p_{trans} \leq 22 \text{ MeV/fm}^3$ generate (connected) hybrid stars with masses larger than $2.5 M_\odot$ for the $m^*/m = 0.60$ case. Since $p_{trans} = 22 \text{ MeV/fm}^3$ is the lowest transitional pressure of category III it is reasonable to assume, that the lower limits of category III in cases with higher effective masses do not generate $2.5 M_\odot$ hybrid stars, even at low jumps in energy density. This assumption proves to be true as can be seen in Fig. 4-5. Only category IV phase transitions (purple

line) come close to such large masses. However, the $m^*/m = 0.60$ case (Fig. 3) generates category III hybrid stars massive enough to reach the mass constraint of $2.14_{-0.09}^{+0.10} M_\odot$ [4] at $\Delta\epsilon \geq 350 \text{ MeV/fm}^3$ and thus visible twin stars. Like for the $m^*/m = 0.55$ case category I and II phase transitions do not generate stars compact enough to fit the GW170817 data.

For the $m^*/m = 0.65$ case depicted in Fig.4 only the lower limit of category III (green line) still meets the $2.14_{-0.09}^{+0.10} M_\odot$ mass constraint before visible twin stars are not possible anymore. In comparison with Fig. 3 the impact of the transitional pressure on the position of the M_2 curve becomes more apparent. Since higher values of the effective mass lead to softer EoSs the transitional pressures corresponding to 1, 1.5 and $2 M_\odot$ rise, leading to lower M_2 curves, that are further apart, than at higher effective masses. The $m^*/m = 0.65$ EoSs is the stiffest case investigated here, that produces neutron stars compact enough to meet the GW170817 measurement without a phase transition. This means, that the highest possible category I configuration compatible with GW170817 is the $M_{max} = 2.15 M_\odot$ case of the $m^*/m = 0.65$ EoS. The differences between the transitional pressures become even more apparent for the effective mass $m^*/m = 0.70$ shown in Fig. 5 where the distances between the different lines increases further. For this case only category IV phase transitions can generate visible twin star EoSs which contain hybrid stars within the $2.14_{-0.09}^{+0.10} M_\odot$ constraint.

We summarize the compatibility of the four categories and the five investigated effective masses in table I. Here the letters a, b, c, d and e stand for the effective masses 0.55, 0.60, 0.65, 0.70 and 0.75 respectively. The appearance of a letter in a cell indicates, that the constraint (row) is fulfilled by the related category (column) for the corresponding effective mass. The brackets indicate, that an effective mass only partially or narrowly fulfills the constraint. In the case of the NICER constraint this applies to all category IV phase transitions, since the majority of them would be excluded by the 1σ constraint of the radius constraint, but not the 2σ interval.

The hypothetical constraint of $2.59_{-0.09}^{+0.08} M_\odot$ would exclude all twin stars and even most connected branches. Apart from that, only the $m^*/m = 0.65$ case fulfills all constraints for all categories. The considerations of the tidal deformability discussed in the context of GW170817 are found in more detail in our previous publication [17], as well as our discussion in regard to the NICER constraint.

	CI	CII	CIII	CIV	Connected
NICER	abcd	abcd	abcd	(abcde)	abcde
GW170817	cd	cd	(a)bcd	abcde	abcde
$2.05 M_\odot$	abcd	abc	abc	abcde	abcde
$2.50 M_\odot$	/	/	/	/	ab

TABLE I. Shown are effective masses that fulfill the constraints for categories of twin stars. The letters a, b, c, d and e correspond to the effective masses 0.55, 0.60, 0.65, 0.70 and 0.75 respectively. We only show the lower limit of the mass constraints from Cromartie et al. [4] and the unknown compact object of GW190814 [18]. It is obvious, that the tidal deformability constraint from GW170817 favors soft EoSs, while the mass constraints favor stiff EoSs. Only the case $m^*/m = 0.65$ fulfills all constraints for all categories, except for GW190814, which can not be fulfilled by any category.

IV. CONCLUSION

We combined the parameterizable relativistic mean field equation of state with a constant speed of sound approach for quark matter to make a general parameterized study about the possible existence of hybrid stars and twin stars. For this investigation we compare the mass-radius relations of EoSs with varying effective nucleon masses m^*/m (and thus varying stiffness) with mass constraints from a hypothetical $2.5 M_\odot$ neutron star and the $2.14_{-0.09}^{+0.10} M_\odot$ neutron star observed by Cromartie et al. [4]. We find that only the cases $m^*/m = 0.55$ and $m^*/m = 0.60$ can generate hybrid stars massive enough to reach $2.5 M_\odot$. However, these configurations would consist of a single mass-radius line with a kink, instead of two separate branches featuring twin stars. Effective masses of $m^*/m \leq 0.65$ can generate visible twin stars with a $0.1 M_\odot$ mass gap that reach the limit of $2.14_{-0.09}^{+0.10} M_\odot$ of Cromartie et al. [4]

Furthermore we considered the tidal deformability constraint from the LIGO measurement of GW170817 [55], which favors soft EoSs that generate compact stars [12–16]. This results in the effective masses $m^*/m = 0.55$ and $m^*/m = 0.60$ being disfavored, unless an early phase transition is present (see [17]). NICERs measurement of J0030+0451 [6–8] suggests a phase transition at masses of at least $1 M_\odot$, as most earlier phase transitions usually generate too small radii [17].

We find, that a mass constraint of $2.5 M_\odot$ would rule out all twin star solutions, as well as most hybrid star solutions. The maximal mass that allows for twin star solutions is about $2.2 M_\odot$, which can be realized for the stiffest EoS in our model at the lowest possible transitional pressure. We also find that for a maximal pulsar mass of $2.15 M_\odot$ and larger a possible phase transition has to be present below neutron star mass configurations of $2 M_\odot$.

ACKNOWLEDGMENTS

J.E.C. thanks the Giersch foundation for their support with a Carlo and Karin Giersch Scholarship.

-
- [1] P. Demorest, T. Pennucci, S. Ransom, M. Roberts, and J. Hessels, *Nature* **467**, 1081 (2010), arXiv:1010.5788 [astro-ph.HE].
- [2] J. Antoniadis, P. C. Freire, N. Wex, T. M. Tauris, R. S. Lynch, M. H. van Kerkwijk, M. Kramer, C. Bassa, V. S. Dhillon, T. Driebe, J. W. T. Hessels, V. M. Kaspi, V. I. Kondratiev, N. Langer, T. R. Marsh, M. A. McLaughlin, T. T. Pennucci, S. M. Ransom, I. H. Stairs, J. van Leeuwen, J. P. W. Verbiest, and D. G. Whelan, *Science* **340**, 6131 (2013), arXiv:1304.6875 [astro-ph.HE].
- [3] E. Fonseca, T. T. Pennucci, J. A. Ellis, and other, *Astrophys. J.* **832**, 167 (2016), arXiv:1603.00545 [astro-ph.HE].
- [4] H. T. Cromartie, S. M. R. E. Fonseca, and e. a. P. B. Demorest, *Nat. Astron.* **4**, 72 (2019), arXiv:1904.06759 [astro-ph.HE].
- [5] L. Nieder *et al.*, *Astrophys. J.* **902**, L46 (2020), arXiv:2009.01513 [astro-ph.HE].
- [6] M. C. Miller, F. K. Lamb, A. J. Dittmann, *et al.*, *Astrophys. J. Lett.* **887**, L24 (2019), arXiv:1912.05705 [astro-ph.HE].
- [7] T. E. Riley, A. L. Watts, S. Bogdanov, *et al.*, *Astrophys. J. Lett.* **887**, L21 (2019), arXiv:1912.05702 [astro-ph.HE].
- [8] G. Raaijmakers, T. E. Riley, A. L. Watts, *et al.*, *Astrophys. J. Lett.* **887**, L22 (2019), arXiv:1912.05703 [astro-ph.HE].
- [9] B. P. Abbott, R. Abbott, T. D. Abbott, *et al.* (Virgo, LIGO Scientific), *Phys. Rev. Lett.* **119**, 161101 (2017), arXiv:1710.05832 [gr-qc].
- [10] E. Annala, T. Gorda, A. Kurkela, and A. Vuorinen, *Phys. Rev. Lett.* **120**, 172703 (2018), arXiv:1711.02644 [astro-ph.HE].
- [11] A. Bauswein, O. Just, H.-T. Janka, and N. Stergioulas, *Astrophys. J.* **850**, L34 (2017), arXiv:1710.06843 [astro-ph.HE].
- [12] V. Paschalidis, K. Yagi, D. Alvarez-Castillo, D. B. Blaschke, and A. Sedrakian, *Phys. Rev. D* **97**, 084038 (2018), arXiv:1712.00451 [astro-ph.HE].
- [13] D. E. Alvarez-Castillo, D. B. Blaschke, A. G. Grunfeld, and V. P. Pagura, *Phys. Rev. D* **99**, 063010 (2019), arXiv:1805.04105 [hep-ph].
- [14] J.-E. Christian, A. Zacchi, and J. Schaffner-Bielich, *Phys. Rev. D* **99**, 023009 (2019), arXiv:1809.03333 [astro-ph.HE].
- [15] G. Montana, L. Tolos, M. Hanauske, and L. Rezzolla, *Phys. Rev. D* **99**, 103009 (2019), arXiv:1811.10929 [astro-ph.HE].
- [16] M. Sieniawska, W. Turczanski, M. Bejger, and J. L. Zdunik, *Astron. Astrophys.* **622**, A174 (2019), arXiv:1807.11581 [astro-ph.HE].
- [17] J.-E. Christian and J. Schaffner-Bielich, *Astrophys. J. Lett.* **894**, L8, arXiv:1912.09809 [astro-ph.HE].
- [18] R. Abbott, T. D. Abbott, S. Abraham, F. Acernese, and e. a. K. Ackley, *The Astrophysical Journal* **896**, L44 (2020).
- [19] M. H. Johnson and E. Teller, *Phys. Rev.* **98**, 783 (1955).
- [20] H.-P. Duerr, *Phys. Rev.* **103**, 469 (1956).
- [21] J. D. Walecka, *Ann. Phys. (N.Y.)* **83**, 491 (1974).
- [22] J. Boguta and A. R. Bodmer, *Nucl. Phys.* **A292**, 413 (1977).
- [23] B. D. Serot and J. D. Walecka, *Adv. Nucl. Phys.* **16**, 1 (1986).
- [24] H. Mueller and B. D. Serot, *Nucl. Phys.* **A606**, 508 (1996), arXiv:nucl-th/9603037 [nucl-th].
- [25] S. Typel, G. Röpke, T. Klähn, D. Blaschke, and H. H. Wolter, *Phys. Rev. C* **81**, 015803 (2010), arXiv:0908.2344 [nucl-th].
- [26] N. Hornick, L. Tolos, A. Zacchi, J.-E. Christian, and J. Schaffner-Bielich, *Phys. Rev. C* **98**, 065804 (2018), arXiv:1808.06808 [astro-ph.HE].
- [27] D. D. Ivanenko and D. F. Kurdgelaidze, *Astrophys. J.* **1**, 251 (1965).
- [28] N. Itoh, *Prog.Theor.Phys.* **44**, 291 (1970).
- [29] M. Alford, M. Braby, M. Paris, and S. Reddy, *Astrophys. J.* **629**, 969 (2005), arXiv:nucl-th/0411016 [nucl-th].
- [30] J. Coelho, C. Lenzi, M. Malheiro, J. Marinho, R.M., and M. Fiolhais, *Int.J.Mod.Phys. D* **19**, 1521 (2010), arXiv:1001.1661 [nucl-th].
- [31] H. Chen, M. Baldo, G. Burgio, and H.-J. Schulze, *Phys.Rev. D* **84**, 105023 (2011), arXiv:1107.2497 [nucl-th].
- [32] K. Masuda, T. Hatsuda, and T. Takatsuka, *Astrophys. J.* **764**, 12 (2013), arXiv:1205.3621 [nucl-th].
- [33] N. Yasutake, R. Lastowiecki, S. Benic, D. Blaschke, T. Maruyama, *et al.*, *Phys.Rev. C* **89**, 065803 (2014), arXiv:1403.7492 [astro-ph.HE].
- [34] A. Zacchi, M. Hanauske, and J. Schaffner-Bielich, *Phys. Rev. D* **93**, 065011 (2016), arXiv:1510.00180 [nucl-th].
- [35] B. Kämpfer, *J.Phys. A* **14**, L471 (1981).
- [36] N. K. Glendenning and C. Kettner, *Astron. Astrophys.* **353**, L9 (2000), astro-ph/9807155.
- [37] K. Schertler, C. Greiner, J. Schaffner-Bielich, and M. H. Thoma, *Nucl. Phys. A* **677**, 463 (2000), astro-ph/0001467.
- [38] J. Schaffner-Bielich, M. Hanauske, H. Stöcker, and W. Greiner, *Phys. Rev. Lett.* **89**, 171101 (2002), astro-ph/0005490.
- [39] J. Zdunik and P. Haensel, *Astron.Astrophys.* **551**, A61 (2013), arXiv:1211.1231 [astro-ph.SR].
- [40] M. G. Alford, G. Burgio, S. Han, G. Taranto, and D. Zappalà, *Phys. Rev. D* **92**, 083002 (2015), arXiv:1501.07902 [nucl-th].
- [41] D. Blaschke and D. E. Alvarez-Castillo, *Proceedings, 11th Conference on Quark Confinement and the Hadron Spectrum (Confinement XI): St. Petersburg, Russia, September 8-12, 2014*, AIP Conf. Proc. **1701**, 020013 (2016), arXiv:1503.03834 [astro-ph.HE].
- [42] A. Zacchi, L. Tolos, and J. Schaffner-Bielich, *Phys. Rev. D* **95**, 103008 (2017), arXiv:1612.06167 [astro-ph.HE].

- [43] M. G. Alford and A. Sedrakian, *Phys. Rev. Lett.* **119**, 161104 (2017), arXiv:1706.01592 [astro-ph.HE].
- [44] J.-E. Christian, A. Zacchi, and J. Schaffner-Bielich, *Eur. Phys. J.* **A54**, 28 (2018), arXiv:1707.07524 [astro-ph.HE].
- [45] D. Blaschke, D. E. Alvarez-Castillo, A. Ayriyan, H. Grigorian, N. K. Lagarni, and F. Weber, “Astrophysical aspects of general relativistic mass twin stars,” (2020) pp. 207–256, arXiv:1906.02522 [astro-ph.HE].
- [46] P. Jakobus, A. Motornenko, R. Gomes, J. Steinheimer, and H. Stoecker, (2020), arXiv:2004.07026 [nucl-th].
- [47] J. L. Zdunik, M. Bejger, P. Haensel, and E. Gourgoulhon, *Astron. Astrophys.* **450**, 747 (2006), astro-ph/0509806.
- [48] M. G. Alford, S. Han, and M. Prakash, *JPS Conf.Proc.* **1**, 013041 (2014).
- [49] M. G. Alford and S. Han, *Eur. Phys. J.* **A52**, 62 (2016), arXiv:1508.01261 [nucl-th].
- [50] H. Tan, J. Noronha-Hostler, and N. Yunes, (2020), arXiv:2006.16296 [astro-ph.HE].
- [51] B. G. Todd-Rutel and J. Piekarewicz, *Phys. Rev. Lett.* **95**, 122501 (2005), arXiv:nucl-th/0504034 [nucl-th].
- [52] W.-C. Chen and J. Piekarewicz, *Phys. Rev.* **C90**, 044305 (2014), arXiv:1408.4159 [nucl-th].
- [53] C. Drischler, A. Carbone, K. Hebeler, and A. Schwenk, *Phys. Rev.* **C94**, 054307 (2016), arXiv:1608.05615 [nucl-th].
- [54] J. Boguta and H. Stöcker, *Physics Letters B* **120**, 289 (1983).
- [55] B. P. Abbott, R. Abbott, T. D. Abbott, *et al.* (LIGO Scientific, Virgo), *Phys. Rev.* **X9**, 011001 (2019), arXiv:1805.11579 [gr-qc].